EXPERIMENTAL OUT-OF-PLANE BEHAVIOUR OF A RAMMED EARTH SUB-ASSEMBLAGE SUBJECTED TO SEISMIC INPUTS

A. Romanazzi[1*], D.V. Oliveira[2], R.A. Silva[3], P.X. Candeias[4], A.C. Costa[5] and A. Carvalho[6]

[1] ISISE, University of Minho, Guimarães, Portugal, aromanazzi89@gmail.com

[2] ISISE, University of Minho, Guimarães, Portugal, danvco@civil.uminho.com

[3] ISISE, University of Minho, Guimarães, Portugal, ruisilva@civiluminho.com

[4] NESDE, LNEC, Lisbon, Portugal, pcandeias@lnec.pt

[5] NESDE, LNEC, Lisbon, Portugal, alf@lnec.pt

[6] NESDE, LNEC, Lisbon, Portugal, xana.carvalho@lnec.pt

*Corresponding author

Abstract

Rammed earth technique is spread worldwide, representing the local identity of many cultures for which they must be preserved. Yet, rammed earth heritage is also well known for its high seismic vulnerability and despite the increasing concern for this aspect, few investigations were conducted on dynamic response of such structures. In this framework, an experimental program was undertaken on a rammed earth mock-up by means of shake table tests carried out at the National Laboratory of Civil Engineering (LNEC) in Lisbon. To investigate the out-of-plane behaviour of rammed earth walls, a mock-up was built in real scale with a U-shape and then subjected to a series of increasing seismic inputs. The results are here discussed in terms of damage, displacements and base shear coefficient. In conclusion, the model behaved as a rigid block to earthquake excitations.

Keywords:

Shake table test, earthen buildings, rammed earth.

1 INTRODUCTION

Rammed earth is one of the most ancient building techniques based on the use of soil, in which a mixture of moistened earth is compacted within a formwork (Silva et al., 2013). Besides monuments (Jaquin Paul A., 2008), rammed earth technique was widely used also for affordable solution in response to the large housing demand, as for example in Alentejo (Southern Portugal), where a considerable vernacular heritage is found (Silva et al., 2018). Yet, rammed earth buildings are also well known for their high seismic vulnerability, which is a consequence of the low mechanical properties of the material, high self-weight and poor connection between structural elements, causing in-plane cracking and out-of-plane mechanism of bearing walls (Bui et al., 2014) (Costa et al., 2015). Even though, a comprehensive investigation on the seismic vulnerability of rammed earth structure is still needed. In fact, mostly static tests on rammed earth were conducted so far (El-Nabouch et al., 2017) (Bui et al., 2016) (Miccoli et al., 2015), while few dynamic tests (Wang et al., 2016) (Reyes et al., 2019) were carried out due to their demanded time, cost, and complexity, although they are the most adequate to investigate the seismic behavior of structures. In this framework, the present investigation addresses the out-of-plane behavior of a U-shape rammed earth mock-up subjected to a shake table tests carried out at the Earthquake Engineering and Structural Dynamics Division (NESDE) of the National Laboratory of Civil Engineering (LNEC) in Lisbon. The overall test protocol considered two phases: 1) dynamic tests, in which the seismic action was applied with increasing amplitude along one direction; 2) dynamic identification tests, to assess the change of the dynamic properties of the mock-up. Hereinafter, the set-up is illustrated, describing the properties of the mock-up and the definition of the inputs. Afterwards, the results of the experimental program are discussed in terms of crack pattern, damage, displacements, and base shear coefficient.

2 EXPERIMENTAL PROGRAM

2.1 Preparation of the mock-up

The geometry of the mock-up was defined to simulate the out-of-plane behaviour of a rammed earth wall; for this reason, the rammed earth model had a U-shape with a wall thickness of 0.50 m and height of 2.20 m. The width of the main wall was 4.60 m, with a free span of 3.60 m, while the two buttresses were 2.00 m long (Fig. 1). In addition, a traditional foundation for rammed earth buildings was realized with a layer of cement mortar with 0.10 m thick, into which limestones were embedded to improve the interlocking between the foundation and the wall. Afterwards, once the mixture of soil was ready, it was poured into a metallic formwork of the same size of the wall and then mechanically compacted in layers of about 0.10 m thickness each, resulting in a monolithic rammed earth wall.

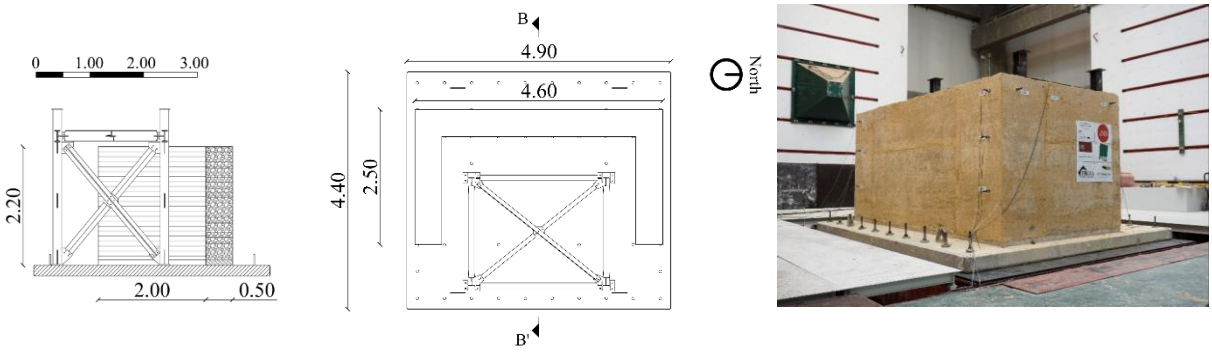

Fig. 1 Geometry of the mock-up

2.2 Set-up of the shake table test

Regarding the seismic input, the generated time histories were based on stochastic methods and a seismological model which consider finite fault effects (Carvalho et al., 1998). Therefore, two different seismogenic faults were assumed, namely Messejana Fault for a near-field scenario, and Horseshoe Fault for a far-field scenario, while the case study was located in Odemira (South of Portugal). Afterwards, the generated accelerograms were applied along the W-E direction and scaled through increasing amplification factors for each step, as reported in Tab. 1. Since a discrepancy might occur between the designed response spectrum (target) and the spectrum obtained from the actual test, each step of seismic input might require few iterations to reduce such difference. For this reason, although the increasing levels of seismic action were 8, the total performed inputs were 31. For the sake of brevity, Tab. 1 summarizes the only seismic step where the test response spectrum (URE-ST-*#number of test*) achieved the target response spectrum. In addition, once the target signal was achieved, a dynamic identification (DI-URE-*#number of test*) was conducted by means of white noise before passing to the next level of seismic intensity.

Tab. 1 Test sequence for RE mock-up

Incremental level	Seismic signal	Generated accelerogram	Scale factor	Dynamic identification
0	-	-	-	DI-URE-01
1	URE-ST-03	Messejana	1	DI-URE-02
2	URE-ST-08	Messejana	1	DI-URE-03
3	URE-ST-12	Ferradura	1	DI-URE-04
4	URE-ST-16	Ferradura	1	DI-URE-05
5	URE-ST-23	Ferradura	1	DI-URE-06
6	URE-ST-26	Ferradura	2	DI-URE-07
7	URE-ST-29	Ferradura	4	DI-URE-08
8	URE-ST-31	Ferradura	8	DI-URE-09

To represent each seismic signal, a series of ground motion parameters were assessed, such as the duration of the ground motion [s], which considers the effective duration of the earthquake, the Peak Ground Acceleration (PGA) [m/s^2], the Peak Ground Velocity (PGV) [m/s] and the Peak Ground Displacement (PGD) [mm]. Such peak values are the maximum values of the amplitude in the time; nonetheless, they are not representative of the entire history of amplitudes of the signal and its effects on the structures. Therefore, further integral parameters which take into account the history of the amplitudes occurring in a time history are calculated as Cumulative Absolute Velocity (CAV), Arias Intensity (AI) and Input Energy (IE) (Cosenza and Manfredi, 2000) (Kramer, 1996). The peak ground values and the seismic properties that consider the entire time histories are illustrated in Fig. 2 and Fig. 3 for the entire test sequence.

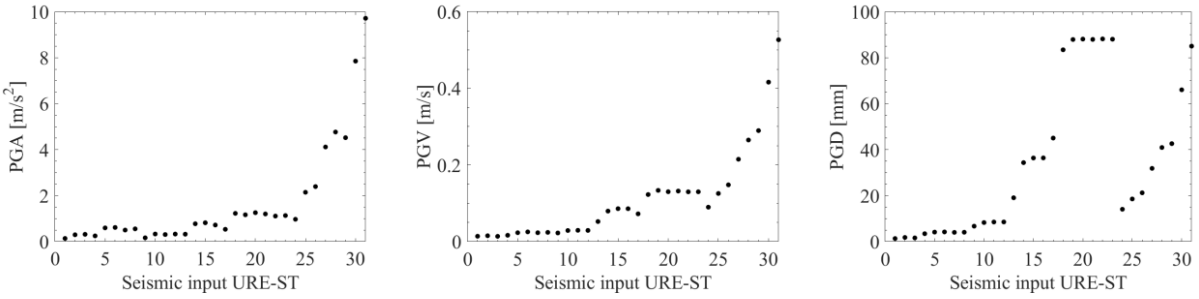

(a) (b) (c)

Fig. 2. Ground motion parameters: a) PGA, b) PGV, and c) PGD

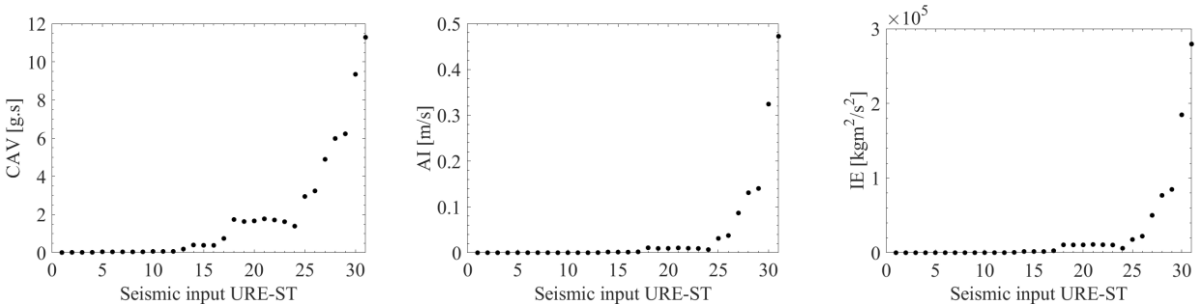

(a) (b) (c)

Fig. 3 Integral parameters of the test sequence: a) CAV, b) AI, and c) IE

To monitor the out-of-plane response of the mock-up, 6 accelerometers were set on the West side of the wall in correspondence to the buttresses (AW01 to AW06), as showed in Fig. 4a, while another 15 accelerometers (AE01 to AE15) were placed on the East side and buttresses (Fig. 4c). Since an out-of-plane collapse with a separation of the corner was hypothesized, further 4 accelerometers were placed on the South façade (AS01 and AS02) and on the North façade (AN01 and AN02), of which one in correspondence of the wall and one at the corner of the buttresses, which allow as well to record local modes (Fig. 4b and Fig. 4c).

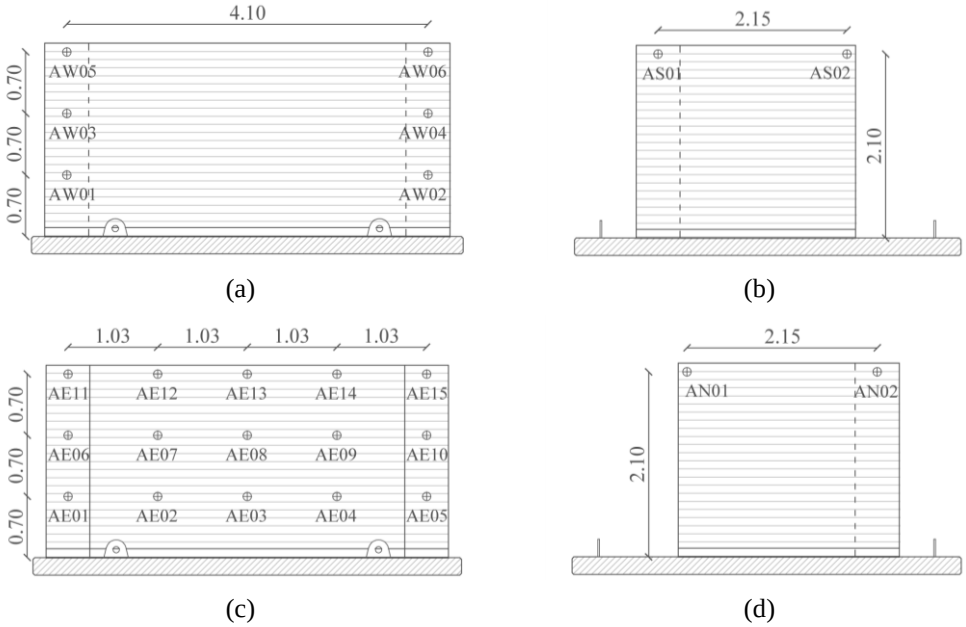

(a) (b) (c) (d)

Fig. 4 Set-up of accelerometers: (a) West, (b) South, (c) East, (d) North

3 RESULTS AND DISCUSSION

3.1 Dynamic identification

With the aim of tracking the progression of damage, the dynamic properties of the mock-up were assessed once the target response spectrum was achieved. The input signal used in the dynamic identification tests corresponds to a band-limited white noise, with enough frequency range and low amplitude, so to avoid any further damage. Following, the results of the dynamic identifications of the entire test sequence are reported in Tab. 2. Although the cracks in the mock-up were evident, no difference was encountered in the natural frequencies of the mock-up between the dynamic identification tests, thus pointing to the absence of stiffness losses. This could be explained by the combination of the fact that the high self-weight of the mock-up closed the horizontal cracks, and that the amplitude of the dynamic identification input signal was not strong enough to reopen them.

Tab. 2 Natural frequencies detected for each dynamic identification

Dynamic Identification	Frequency 1 [Hz]	Frequency 2 [Hz]	Frequency 3 [Hz]	Frequency 4 [Hz]	Frequency 5 [Hz]
DI-URE-01	14.40	22.38	23.79	25.78	31.82
DI-URE-02	14.43	22.78	23.80	25.83	31.90
DI-URE-03	14.21	22.55	23.83	25.75	31.41
DI-URE-04	14.19	22.37	23.83	25.80	31.80
DI-URE-05	14.17	22.18	23.81	25.75	31.52
DI-URE-06	13.92	22.08	23.80	25.65	31.19
DI-URE-07	13.78	22.41	23.80	25.59	30.77
DI-URE-08	13.60	22.05	23.75	25.43	30.19
DI-URE-09	13.75	21.92	23.76	25.05	29.96

3.2 Displacement profile

The envelope profiles are here reported. In particular, Fig. 5 and Fig. 6 report the envelope of the top horizontal profiles (AE11 to AE15) and the vertical profiles considering the middle section of the wall (AE03-AE08-AE13), for which both positive (toward West) and negative (toward East) values were considered. For the sake of clarity in visual representation, the graphs are reported for the last six signal inputs of the test sequence (URE-ST-26 to URE-ST-31), as the displacements achieved appreciable values. As expected, the out-of-plane displacements increased with the increasing of the intensity of the seismic actions, achieving a maximum value at the last seismic input of about 15 mm towards West direction (Fig. 5a), while the vertical profiles of the wall highlight the out-of-plane rigid rotation of the wall (Fig. 6).

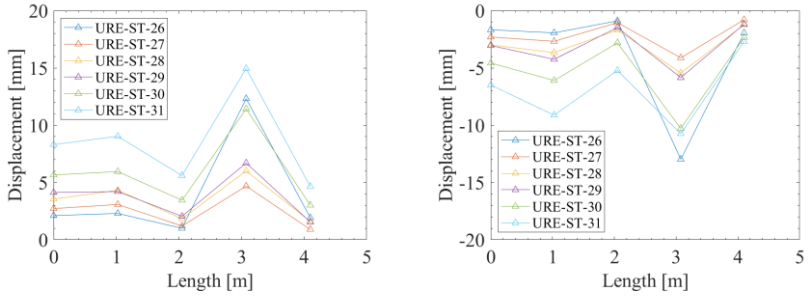

(a) (b)

Fig. 5 Envelope of the top horizontal profile a) positive displacements, b) negative displacements

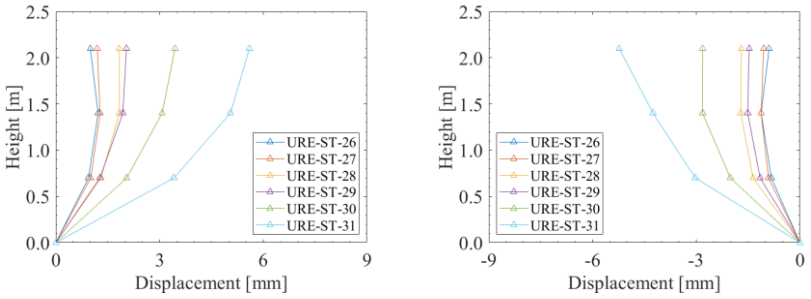

Fig. 6 Envelope of the main wall vertical profile: a) positive displacements, and b) negative displacements

3.3 Base shear coefficient

In what concerns the base shear force (BSF) during the seismic tests, in a single degree of freedom, it can be estimated by the elastic resisting force, $F_S(t)$, in opposite phase with the inertial forces, $F_I(t)$, assuming that the damping resisting forces, $F_D(t)$, are zero at the maximum of $F_S(t)$ (Beyer et al., 2014) (Candeias Paulo J., 2008). Since the accelerations on the mock-up are measured on some points, assuming that the mass remains constant, the BSF is the sum of the inertial forces of a discrete lumped system as (Beyer et al., 2014):

$$BSF(t) = \sum_{i=1}^{n} -F_{I_i}(t) = -\sum_{i=1}^{n} m_i \ddot{u}_i(t) \quad (1)$$

where $F_{I,i}(t)$ is the inertial force, m_i is the assigned mass and $\ddot{u}(t)$ is the measured acceleration at point i. From here, the Base Shear Coefficient (BSC) is evaluated by normalizing the BSF by the self-weight of the mock-up. Following, the maximum values of BSC are discussed as a function of PGA (Fig. 7a), CAV (Fig. 7b), AI (Fig. 7c), and IE (Fig. 7d). As illustrated in Fig. 7a, and Fig. 7b, a linear relationship with high coefficient of correlation (R^2=0.98 ~ 0.99) can be found when the PGA or CAV are considered as input, while quadratic correlation with high coefficient of correlation (R^2=0.98 ~ 0.99) was found analysing the maximum BSC against the IA, and IE (Fig. 7c and Fig. 7d). The results above presented might suggest that the properties of input which take into account the duration and the content of frequency of the earthquake, as IA and IE, are more suitable to describe the inelastic response of the structure in terms of base shear coefficient, which can reach a capacity of 1.07.

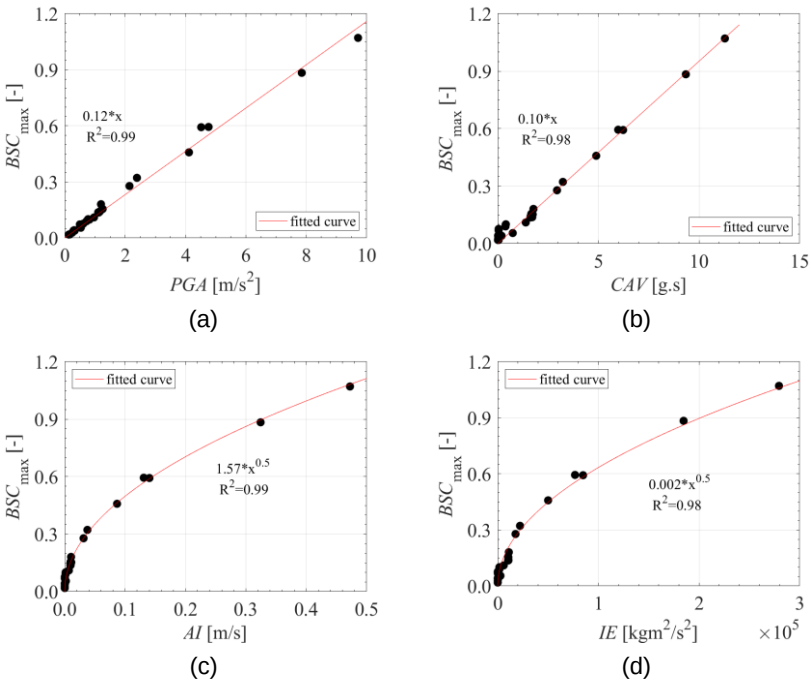

Fig. 7 Regression analyses between maximum BSC and: a) PGA, b) CAV, c) AI, and d) IE

4 CONCLUSION

The first outcomes of a series of shake table tests on a rammed earth mock-up are here presented. The fact that the dynamic identification tests did not report changes in vibration frequencies indicate that such tests may not be appropriate for damage detection in this kind of structures. This could be due to the high self-weight of the wall which closed the horizontal crack, combined with the low amplitude motions used in such tests. With regard to the displacements, the horizontal and vertical envelope profiles demonstrated the out-of-plane overturning of the wall as a rigid block. Linear and quadratic correlations were found between seismic parameters and BSC allowing to predict the seismic performance of the mock-up.

Finally, the present work represents the base for an ongoing calibration of a numerical model, which will provide further insight about the damage and seismic performance of rammed earth structures.

5 ACKNOWLEDGEMENTS

This work was partly financed by FEDER funds through the Operational Programme Competitiveness Factors (COMPETE 2020) and by national funds through the Foundation for Science and Technology (FCT) within the scope of project SafEarth - PTDC/ECM-EST/2777/2014 (POCI-01-0145-FEDER-016737). The support from grants SFRH/BD/131006/2017 and SFRH/BPD/97082/2013 is also acknowledged. Acknowledgments are addressed to the Earthquake Engineering and Structural Dynamics Division (NESDE) of the National Laboratory of Civil Engineering (LNEC) in Lisbon and to João Bernardino, Lda. and TERRACRUA - Construções Ecológicas Unipessoal, Lda for building the rammed earth model.

6 REFERENCES

Beyer, K., Tondelli, M., Petry, S., Peloso, S., 2014. Seismic response of a 4-storey building with reinforced concrete and unreinforced masonry walls. In: Proceeding of the 9th International Masonry Conference, Guimarães, Portugal.

Bui, T.T., Bui, Q.B., Limam, A., Maximilien, S., 2014. Failure of rammed earth walls: From observations to quantifications. Construction and Building Materials, 51, 295-302.

Bui, T.T., Mesbah, A., Maximillien, S., and Limam, A., 2016. Behavior of rammed earth walls under compression or shear stress. Journal of Materials and Environmental Science, 7, 3584-3594.

Candeias, Paul J., 2008. Seismic vulnerability assessment of masonry buildings (Avaliação da vulnerabilidade sísmica de edifícios de alvenaria) (PhD Thesis), University of Minho, Portugal.

Carvalho, E.C., Bisch, P., Labbe, A., and Pecker, A., 1998. Seismic testing of structures. In: Proceeding of the 11th European conference on earthquake engineering, Paris, France.

Cosenza, E., and Manfredi, G., 2000. Damage indexes and damage measures. Progress in Structural Engineering and Materials, 2, 50-59.

Costa, A.A., Varum, H., Rodrigues, H., Vasconcelos, G., 2015. Seismic behaviour analysis and retrofitting of a row building. In Correia M, Lourenço PB, Varum H, Seismic Retrofitting: Learning from vernacular architecture. London, Taylor and Francis Group.

El-Nabouch, R., Bui, Q.B., Plé, O., and Perrotin, P., 2017. Assessing the in-plane seismic performance of rammed earth walls by using horizontal loading tests. Engineering Structures, 145, 153-161.

Jaquin Paul A. (2008) Analysis of historic rammed earth construction. (PhD thesis) Durham University, United Kingdom.

Kramer, S., 1996. Geotechnical earthquake engineering. Prentice-Hall International Series in Civil Engineering and Engineering Mechanics.

Miccoli, L., Oliveira, D.V., Silva, R.A., Müller, U., and Schueremans, L., 2015. Static behaviour of rammed earth: experimental testing and finite element modelling. Materials and Structures, 48, 3443-3456.

Reyes, J.C., Smith-Pardo, P., Yamin, L.E., Galvis, F.A., Angel, C.C., Sandoval, J.D., Gonzalez, C.D., 2019. Seismic experimental assessment of steel and synthetic meshes for retrofitting heritage earthen structures. Engineering Structures, 198, 109477.

Silva, R.A., Mendes, N., Oliveira, D.V., Romanazzi, A., Domínguez-Martínez, O., Miranda, T., 2018. Evaluating the seismic behaviour of rammed earth buildings from Portugal: from simple tools to advanced approaches. Engineering Structures, 157, 144-156.

Silva, R.A., Oliveira, D.V., Miranda, T., Cristelo, N., Escobar, M.C., Soares, E., 2013. Rammed earth construction with granitic residual soils: The case study of northern Portugal. Construction and Building Materials, 47, 181-191.

Wang, Y., Wang, M., Liu, K., Pan, W., Yang, X., 2016. Shaking table tests on seismic retrofitting of rammed-earth structures. Bulletin of Earthquake Engineering, DOI 10.1007/s10518-016-9996-2.